ELSEVIER

Cement & Concrete Composites 26 (2004) 339–345

Cement & Concrete Composites

www.elsevier.com/locate/cemconcomp

A new method for determination of chloride flux in cement-based materials from chronoamperometry

A. Aït-Mokhtar [a], O. Amiri [a,*], O. Poupard [a,b], P. Dumargue [a]

[a] *LEPTAB, University of La Rochelle, Avenue Michel Crépeau, 17042 La Rochelle Cedex 1, France*
[b] *Chalmers University of Technology, SE-41296 Gothenburg, Sweden*

Abstract

A new method for exploitation of chloride electrodiffusion test is proposed in this work. This method allows calculating chloride flux through a porous medium in steady state by using current transfer with basic electrolyte (without NaCl) and with total electrolyte (after NaCl addition). Currents are obtained experimentally from chronoamperometry. Comparisons of results obtained by this new model with those obtained by a classical dosage of chlorides in the downstream solution of the cell were carried out for three compositions of cement pastes. The results of the model seem to be closer to those of experimental dosage. This preliminary work shows that it is not necessary to measure chloride concentration in upstream or downstream cell, but a simple chronoamperometry suffices to obtain chloride flux, hence the diffusion of chloride ions.

Keywords: Chronoamperometry; Chloride diffusion; Cement-based materials; Mercury porosimetry; Modelling

1. Introduction

The penetration of chlorides in concrete is the main physicochemical process that reduces the service life of reinforced structures by corrosion of steel bars. To characterise the material resistance to the diffusion of these ions, one has to know their flux or their diffusion coefficient through the material.

Considering the slowness of the diffusion phenomenon in cement-based materials, migration tests were developed in laboratories to accelerate the process [1–6]. In steady state, the measurement of the chloride concentration in the anodic cell allows calculating chloride flux and diffusion coefficient by using Fick's second law. Recently, Truc et al. [7] suggested a new technique for the determination of flux and diffusion coefficient. It consists in measuring the drop in the chloride concentration in the cathodic cell. The main advantage of this technique consists in shortening the migration test. However, the dosage requires a heavier experimental procedure, whether if it is upstream or downstream. Furthermore, some phenomena could disturb these measurements. For downstream dosage, Prince et al. [8] had noticed the possibility of oxidation of chloride that results in chlorine (or hypochlorite) in the cathodic cell if the applied electrical field is strong enough. For upstream dosage, because of measurement range, successive dilutions of the sampled solutions are necessary before their dosage; otherwise, these operations could cause inaccuracies.

Moreover, several works had noticed the presence of electrical double layer at the charged surface of porous medium [9,10]. Thus, to take into account the double layer effects and to avoid the inaccuracies of chloride dosage, the aim of this paper is to propose a new method for calculating the chloride flux by using chronoamperometry.

2. Theoretical considerations

The electrodiffusion test requires an electrolyte support (or basic electrolyte: NaOH and KOH) placed in the two compartments of the cell [11]. In this study, the basic electrolyte is a solution of 0.083 M KOH and 0.025 M NaOH. First, an electrical field of 300 V/m was applied between the sides of the sample supposed saturated. So, the convection can be neglected. Chlorides

* Corresponding author. Tel.: +33-5-4645-7230/8203; fax: +33-5-4645-8241.
E-mail address: oamiri@univ-lr.fr (O. Amiri).

0958-9465/$ - see front matter © 2003 Elsevier Ltd. All rights reserved.
doi:10.1016/S0958-9465(03)00008-8

were added and solutions were renewed after reaching balanced transfer. Solutions were also renewed after reaching balanced transfer with NaCl. This procedure allows measuring transfer currents in steady state with basic electrolyte and with total electrolyte (after NaCl addition).

By considering irreversible process theory, vectors of current density due to the cations (k), and the anions (l) contained in the basic electrolyte are:

$$\vec{i}_{\mathrm{P}} = -F\sum_{k=1}^{s} Z_k D_k \,\mathrm{grad}\vec{}\, C_k + \frac{F^2}{RT}\left(\sum_{k=1}^{s} Z_k^2 D_k C_k\right)\vec{E} \tag{1}$$

$$\vec{i}_{\mathrm{N}} = F\sum_{l=1}^{p} Z_l D_l \,\mathrm{grad}\vec{}\, C_l + \frac{F^2}{RT}\left(\sum_{l=1}^{p} Z_l^2 D_l C_l\right)\vec{E} \tag{2}$$

where $\vec{E}$: local electrical field, R: gas constant, T: the absolute temperature, F: Faraday constant, D_k, D_l: diffusion coefficient of cations and anions, respectively, C_k, C_l: cations and anions concentrations, respectively, Z_k, Z_l: cations and anions valence, respectively.

The NaCl in the catholyte is decomposed to ions Na^+ and Cl^-, generating current densities:

$$\vec{i}_{\mathrm{Na^+}} = -FD_{\mathrm{Na^+}} \,\mathrm{grad}\vec{}\, C_{\mathrm{Na^+}} + \frac{F^2 D_{\mathrm{Na^+}}}{RT} C_{\mathrm{Na^+}}\vec{E} \tag{3}$$

$$\vec{i}_{\mathrm{Cl^-}} = FD_{\mathrm{Cl^-}} \,\mathrm{grad}\vec{}\, C_{\mathrm{Cl^-}} + \frac{F^2 D_{\mathrm{Cl^-}}}{RT} C_{\mathrm{Cl^-}}\vec{E} \tag{4}$$

We define:

$$\vec{i}_{\mathrm{T}} = (\vec{i}_{\mathrm{P}} + \vec{i}_{\mathrm{Na^+}}) + (\vec{i}_{\mathrm{N}} + \vec{i}_{\mathrm{Cl^-}}) \quad \text{and}$$
$$\vec{i}^{*}_{\mathrm{T}} = (\vec{i}_{\mathrm{P}} + \vec{i}_{\mathrm{Na^+}}) - (\vec{i}_{\mathrm{N}} + \vec{i}_{\mathrm{Cl^-}}) \tag{5}$$

referred to current densities, total and conjugate, respectively.

We note:

$$\vec{i}^{*}_{\mathrm{B}} = \gamma_{\mathrm{B}}\vec{i}_{\mathrm{B}} \quad \text{and} \quad \vec{i}^{*}_{\mathrm{T}} = \gamma_{\mathrm{T}}\vec{i}_{\mathrm{T}} \tag{6}$$

γ_{B}, γ_{T} represent the ratio between the current density and its conjugate for the basic and total electrolyte, respectively.

To take into account the electrical double layer, space charge densities ρ, ρ_{S} and conductivities σ_{B}, σ_{S}, due to the basic electrolyte and to NaCl addition, were introduced, respectively:

$$\begin{aligned}\rho_{\mathrm{B}} &= F\left[\sum_{k=1}^{s} Z_k C_k - \sum_{l=1}^{p} Z_l C_l\right] = F(C_{\mathrm{P}} - C_{\mathrm{N}})\\ \rho_{\mathrm{S}} &= F(C_{\mathrm{Na^+}} - C_{\mathrm{Cl^-}})\end{aligned} \tag{7}$$

$$\begin{aligned}\sigma_{\mathrm{B}} &= \frac{F^2}{RT}\left[\sum_{k=1}^{s} Z_k^2 D_k C_k + \sum_{l=1}^{p} Z_l^2 D_l C_l\right]\\ &= \frac{F^2}{RT}(\alpha_{\mathrm{P}} D_{\mathrm{P}} C_{\mathrm{P}} + \alpha_{\mathrm{N}} D_{\mathrm{N}} C_{\mathrm{N}})\\ \sigma_{\mathrm{S}} &= \frac{F^2}{RT}(D_{\mathrm{Na^+}} C_{\mathrm{Na^+}} + D_{\mathrm{Cl^-}} C_{\mathrm{Cl^-}})\end{aligned} \tag{8}$$

C_{P}, C_{N}, α_{P}, α_{P}, D_{P}, D_{N} are defined in the Appendix A.

Vectors $\vec{i}_{\mathrm{T}}$ and $\vec{i}^{*}_{\mathrm{T}}$ become then:

$$\begin{aligned}\vec{i}_{\mathrm{T}} = {} & -D[\mathrm{grad}\vec{}\,\rho_{\mathrm{B}} + \beta\,\mathrm{grad}\vec{}\,\sigma^{*}_{\mathrm{B}} + \lambda_{\mathrm{S}}\{\mathrm{grad}\vec{}\,\rho_{\mathrm{S}} + \beta_{\mathrm{S}}\,\mathrm{grad}\vec{}\,\sigma^{*}_{\mathrm{S}}\}]\\ & + D(\sigma^{*}_{\mathrm{B}} + \lambda_{\mathrm{S}}\sigma^{*}_{\mathrm{S}})\vec{E}^{*}\end{aligned} \tag{9}$$

$$\begin{aligned}\vec{i}^{*}_{\mathrm{T}} = {} & -D[\mathrm{grad}\vec{}\,\sigma^{*}_{\mathrm{B}} + \lambda_{\mathrm{S}}\,\mathrm{grad}\vec{}\,\sigma^{*}_{\mathrm{S}}] + D[(\rho_{\mathrm{B}} + \beta\sigma^{*}_{\mathrm{B}})\\ & + \lambda_{\mathrm{S}}(\rho_{\mathrm{S}} + \beta_{\mathrm{S}}\sigma^{*}_{\mathrm{S}})]\vec{E}^{*}\end{aligned} \tag{10}$$

The parameters D, β, β_{S}, σ^{*}_{B}, σ^{*}_{S}, λ_{S}, E^{*} are defined in the Appendix A.

After defining local transfer equations, this approach consists in establishing macroscopic transfer equations at the scale of porous medium [11], with the aim to determine the transfer current due solely to chloride diffusion. Using the microstructural characteristics of the material, was carried out the transition from local transfer equations to macroscopic transfer equations: mainly the porosity and pore radius ($R_{p\max}$) corresponding to the peak in the pore size distribution. These properties are obtained by mercury intrusion porosimetry (MIP) [12] (see Experimental section). Let us note by $[i]_{\mathrm{B}}$, $[i]_{\mathrm{T}}$, $[i^{*}]_{\mathrm{B}}$, $[i^{*}]_{\mathrm{T}}$ the macroscopic current densities and their conjugates in the basic and total electrolytes, respectively.

After theoretical developments, current densities are linked to conductivities by:

$$\begin{aligned}\frac{\mathrm{d}\ln\sigma_{\mathrm{B}}}{\mathrm{d}z} = [i]_{\mathrm{B}}\Bigg[& \gamma_{\mathrm{B}}\frac{f_1(\sigma_{\mathrm{B}},z) - \beta f_2(\sigma_{\mathrm{B}},z)}{1-\beta^2}\\ & + \frac{f_2(\sigma_{\mathrm{B}},z) - \beta f_1(\sigma_{\mathrm{B}},z)}{1-\beta^2}\Bigg]\end{aligned} \tag{11}$$

for the basic electrolyte, and:

$$\frac{\mathrm{d}\sigma_{\mathrm{S}}}{\mathrm{d}z} = \frac{[i]_{\mathrm{T}}\left[\gamma_{\mathrm{T}}\frac{f_1(\sigma_{\mathrm{S}},z)-\beta_{\mathrm{T}}f_2(\sigma_{\mathrm{S}},z)}{1-\beta_{\mathrm{T}}^2} + \frac{f_2(\sigma_{\mathrm{S}},z)-\beta_{\mathrm{T}}f_1(\sigma_{\mathrm{S}},z)}{1-\beta_{\mathrm{T}}^2}\right]}{\left[(\sigma_{\mathrm{B}} + \sigma_{\mathrm{S}}) - \frac{\beta_{\mathrm{T}}(\beta-\beta_{\mathrm{S}})}{(\sigma_{\mathrm{B}}+\sigma_{\mathrm{S}})}\right]} \tag{12}$$

for the total electrolyte.

Where z is the space variable, $f_1(\sigma_{\mathrm{B}},z)$ and $f_2(\sigma_{\mathrm{B}},z)$ are defined in the Appendix A, σ_{S} is the conductivity due to the NaCl addition, $\sigma_{\mathrm{S}} = \sigma_{\mathrm{T}} - \sigma_{\mathrm{B}}$; σ_{T} is the conductivity due to the total electrolyte.

Eqs. (11) and (12) are solved numerically according to the methodology illustrated in Fig. 1. In this resolution $[i]_{\mathrm{B}}$ and $[i]_{\mathrm{T}}$ are the inputs of the model; they are given by experiments (see next section). The parameters γ_{B}, γ_{T} are the outputs of the model.

According to Amiri [11], the total macroscopic current density and its conjugate are:

- in the basic electrolyte:

$$\begin{aligned}[i]_{\mathrm{B}} &= i_{\mathrm{P}} + i_{\mathrm{N}}\\ [i^{*}]_{\mathrm{B}} &= i_{\mathrm{P}} - i_{\mathrm{N}}\end{aligned} \tag{13}$$

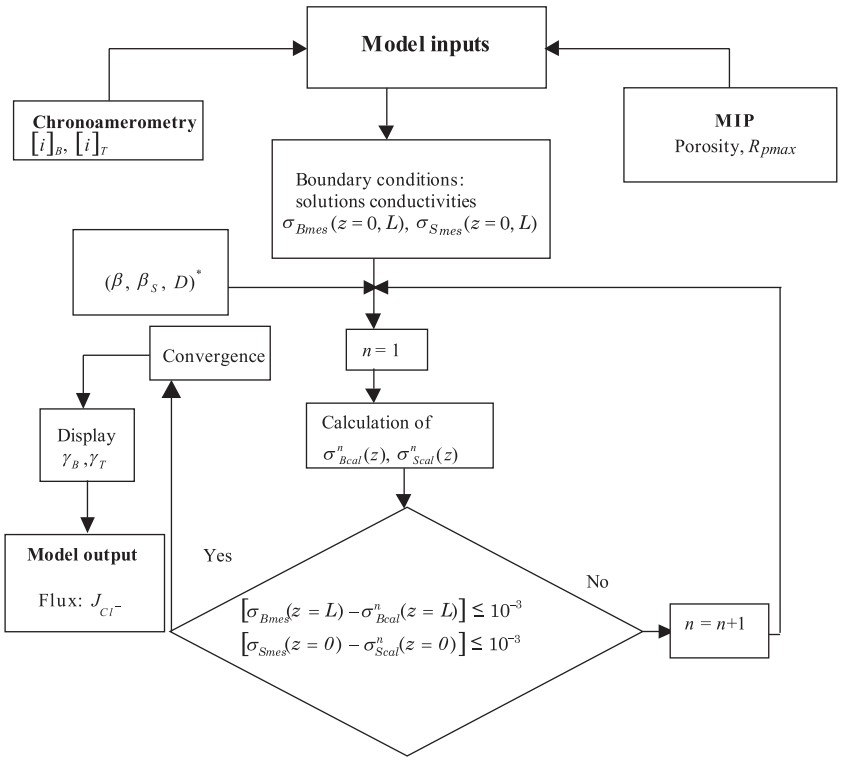

Fig. 1. Simplified view of resolution methodology. (∗: These parameters are calculated from literature data, see relationships in the appendix.)

- after NaCl addition:

$$[i]_T = i_P + i_N + i_{Na^+} + i_{Cl^-}$$
$$[i^*]_T = i_P - i_N + i_{Na^+} - i_{Cl^-} \quad (14)$$

From Eqs. (6), (13) and (14), we have:

$$i_{Cl^-} = \frac{(1-\gamma_T)[i]_T - (1-\gamma_B)[i_z]_B}{2} \quad (15)$$

Flux and current density are linked by a proportionality relationship:

$$J_{Cl^-} = \frac{i_{Cl^-}}{Z_{Cl^-}F} \quad (16)$$

then:

$$J_{Cl^-} = \frac{(1-\gamma_T)[i]_T - (1-\gamma_B)[i_z]_B}{2Z_{Cl^-}F} \quad (17)$$

3. Experimental approach

3.1. Materials and procedure

Three types of cement paste samples with different w/c were manufactured. The cement used is of type CEM-I52.5 according to European Norms (EN197-1). Its chemical composition is given in Table 1.

The specimens had a prismatic form ($12 \times 12 \times 20$ cm^3). After demoulding (24 h after manufacturing), the specimens were cured during 28 days in an alkaline solution, which is identical to that of the electrodiffusion test solution (0.083 M KOH and 0.025 M NaOH). This curing was carried out in order to reduce leaching phenomena.

To avoid wall effects, samples used in electrodiffusion tests were obtained by a technique of core sampling in order to have a cylindrical form with 6.5 cm diameter and 1 cm thickness. The lateral surface was covered with a resin to ensure a unidirectional transfer. Fig. 2 is a schematic view of the experimental set-up.

3.2. Chronoamperometry

The electrodiffusion cell contains two compartments: upstream (2*l*) and downstream (1*l*), filled with the basic solution and separated by the test sample. Four electrodes were used for applying the constant electrical field (300 V/m). Two platinum mesh electrodes were placed

Table 1
Chemical composition of the cement used

CaO	SiO_2	Al_2O_3	Fe_2O_3	MgO	K_2O	Na_2O	SO_3	TiO_2	MnO	S_rO	P_2O_5
64.02	19.81	5.19	2.38	0.9	1.11	0.06	3.5	0.28	0.05	0.15	0.16

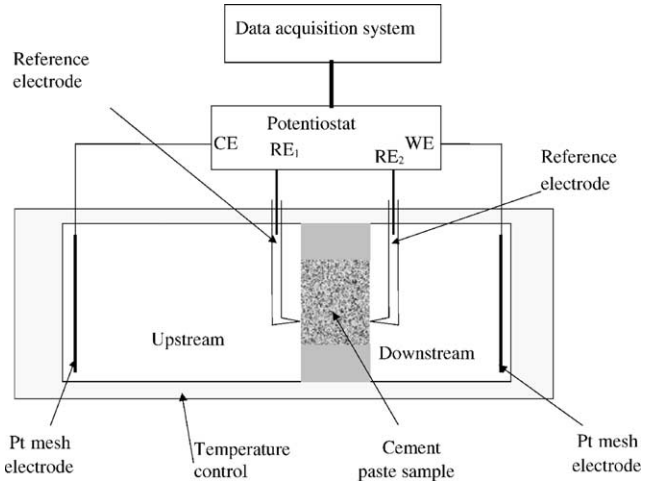

Fig. 2. Schematic view of electrodiffusion cell.

on the extremities of the cell. They are larger than the sample surface to obtain uniform current densities. The two reference electrodes (saturated electrodes calomel) were placed on the sample extremities in order to maintain constant the applied electrical field. The electrodiffusion tests were carried out in the following steps:

- introduction of NaOH and KOH solution in the cell and application of the electrical field,
- renewing the upstream and downstream solutions after current stabilisation,
- reading the $[i]_B$ value (see Table 2) after current stabilisation and renewing upstream and downstream solutions with NaCl (0.5 M) in the upstream compartment,
- renewing the upstream and downstream solutions after current stabilisation,
- reading the $[i]_T$ value (see Table 2) after current stabilisation.

Renewal of the upstream and the downstream solutions was carried out according to their variation in conductivity, e.g. every 10–15 h on average, until obtaining the steady state. The evolution of current density for the tested samples is shown in Fig. 3.

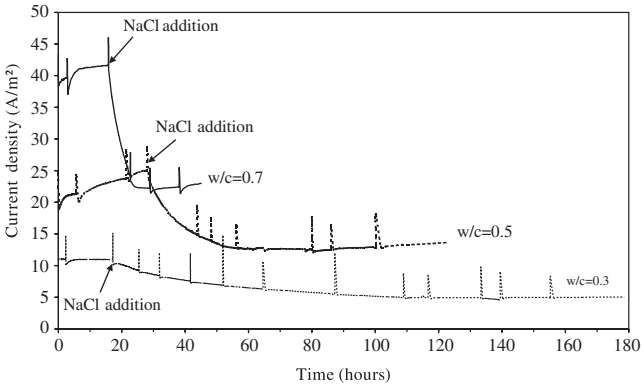

Fig. 3. Chronoamperometry of cement pastes.

3.3. Flux measurements

In parallel with the study of the current density evolution, chlorides were dosed in the downstream compartment by one of the most reliable methods, potentiometric titration [13]. It consists in comparing the measured potential between two electrodes in a solution of unknown Cl^- concentration with those given by a calibration curve. This later is plotted from potentials measured in solutions of known Cl^- concentrations. To measure Cl^- concentration, a chloride ion selective electrode was used in combination with a reference electrode. The two electrodes were connected to a millivoltmeter. The increase in time of these concentrations allows calculating experimental chloride flux J_{mes} crossing the sample in steady state by:

$$J_{mes} = \frac{V_a}{S}\frac{\Delta C}{\Delta t} \tag{18}$$

where V_a: volume of the anodic cell, S: section of the sample, ΔC: increase in the concentration according to the time interval Δt.

Table 2
Experimental and modelling results

Samples			$w/c = 0.3$	$w/c = 0.5$	$w/c = 0.7$
Entry of the model (experimental data)	MIP tests	Porosity (%)	17.76	18.22	28.74
		$R_{p\max}$ (μm)	0.02	0.04	0.055
	Chronoamperometry	$[i]_B$ (A m^{-2})	11	25	42
		$[i]_T$ (A m^{-2})	5	13.5	24
Model output	Model parameters	γ_B	−0.48	−0.48	−0.48
		γ_T	−2.18	−1.29	−1.01
	Theoretical flux and diffusion coefficient	$J_{Cl^-} \times 10^{-5}$ (M m^{-2} s^{-1})	0.61	3.15	7.21
		$D_{Cl^-} \times 10^{-12}$ (m^2 s^{-1})	1.17	5.50	12.64
Experimental validation	Experimental flux and diffusion coefficient	$J_{mes} \times 10^{-5}$ (M m^{-2} s^{-1})	0.78	3.42	7.72
		$D_{mes} \times 10^{-12}$ (m^2 s^{-1})	1.36	5.95	13.40

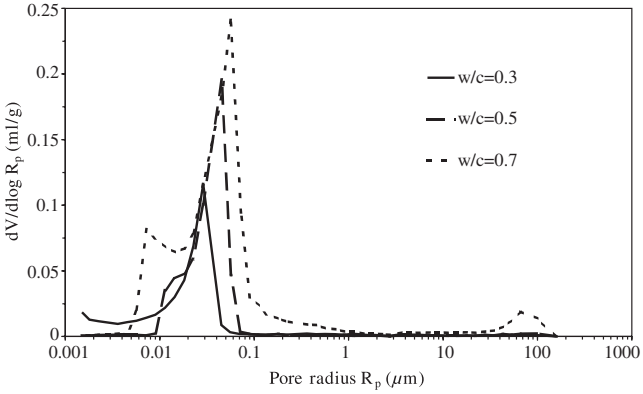

Fig. 4. Pore size distribution for tested materials.

By referring to Amiri et al. [14], the diffusion coefficient is given by:

$$D = \frac{RTL}{Z_{Cl^-}FU}\frac{J}{C_{up}}\left(1 - e^{-\frac{Z_{Cl^-}F}{RT}U}\right) \quad (19)$$

where L: sample thickness, U: difference of potential between the sides of the sample, C_{up}: chloride concentration in the upstream compartment of the migration cell, $C_{up} = 0.5$ M, J: chloride flux.

To validate the model, the 'theoretical' flux J_{Cl^-} (Eq. 17) and diffusion coefficient D_{Cl^-} are compared with 'experimental' flux J_{mes} (Eq. 18) and diffusion coefficient D_{mes}, respectively. Then, in Eq. (19), D is calculated once from J_{Cl^-} and another time from J_{mes}. Results are given in Table 2.

3.4. Mercury intrusion porosimetry test

This test was carried out in order to quantify porosity and $R_{p\max}$ which are the inputs of the model. Samples were taken from the interior of specimens 28 days after manufacturing and then dried for 24 h at 70 °C. Mercury injection measurements were performed with a micromeritics porosimeter (Autopore III 9420) with a pressure range larger than 400 MPa. Results are given in Fig. 4.

4. Electrodiffusion tests results and discussion

Currents densities values in steady state are given in Table 2 with the main results of experimental and modelling.

First, peaks in Fig. 3 are due to solutions renewals during the test. We remark that the density of current decreases until reaching steady state, which corresponds to the constancy of current. Bretton et al. [15] explained the decreasing of current by ionic desaturation phenomenon in the pore solution. This explanation seems to be likely. Indeed, the applied electrical field could compel different ions (contained in pore solution and due to cement composition) to exit from the sample. In fact, the curing of the samples in basic solution (0.083 M KOH and 0.025 M NaOH) does not ensure a complete avoiding of probable leaching phenomena.

Fig. 3 shows that the duration of the experiment is linked to the ratio w/c. In fact, from the moment corresponding to the NaCl addition, the steady state is reached after about 12, 34 and 100 h for the samples $(w/c = 0.7)$, $(w/c = 0.5)$ and $(w/c = 0.3)$, respectively (Fig. 5).

We see in Figs. 5 and 6 that current values increase with the w/c ratio, which is linked with the porosity. The more w/c ratio is high, the more porosity and currents values are high, and lower is the material's resistivity.

According to the modelling, the parameters γ_B and γ_T are linked to the conductivity of the solution. With the basic electrolyte, transfers occur between a balanced solutions (upstream and downstream ones). Then γ_B is constant whatever the material. With the total electrolyte, NaCl addition generates a conductivity gradient between upstream solution (with NaCl) and the sample and another gradient between the sample and downstream solution. That is what makes γ_T change. This parameter seems to be linked to the porous properties of the material, i.e. to the w/c ratio (Fig. 7).

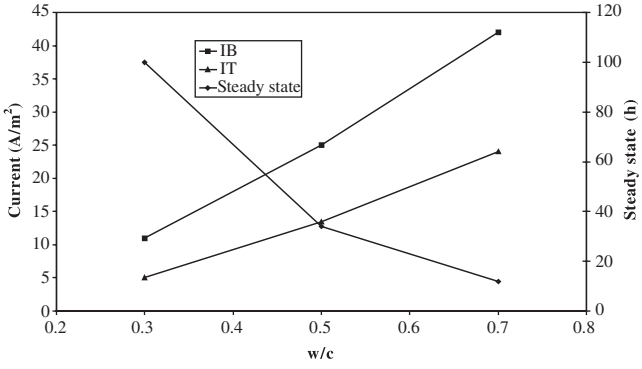

Fig. 5. Current densities and steady state time versus w/c ratio.

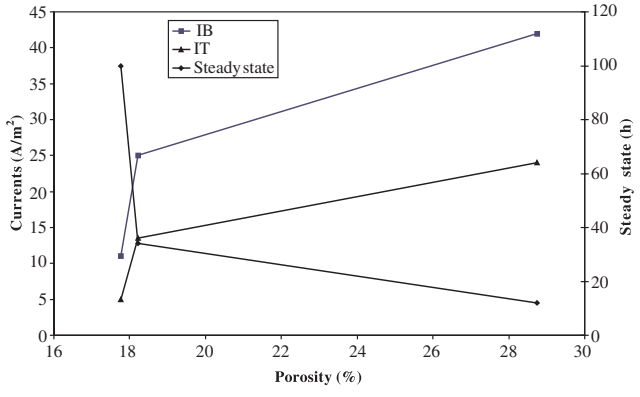

Fig. 6. Current densities and steady state time versus porosities.

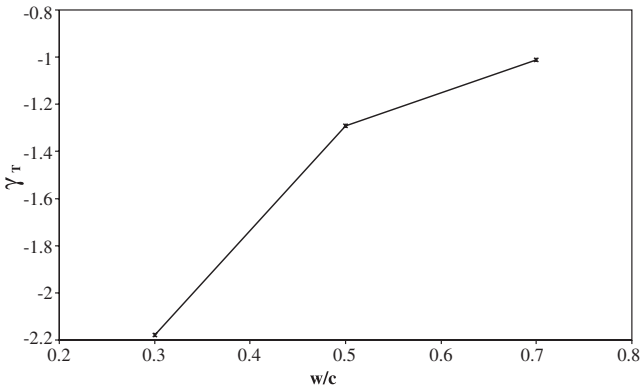

Fig. 7. Evolution of γ_T parameter according to w/c ratio.

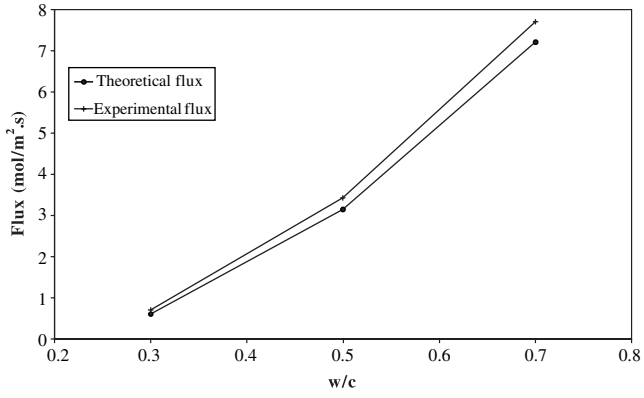

Fig. 8. Comparison between measured and calculated flux.

The comparison between the experimental flux and the theoretical one that calculated by the model (Fig. 8) shows that values measured and calculated are closer for all the samples tested. However, direct measurements of electrical double layer capacity will allow a better adjustment of the parameters γ_B and γ_T given by the numerical resolution. Indeed, in this modelling, for lack of C_{SH} values for cement-based materials, that of silica was used. One will thus obtain 'theoretical' flux even closer to experimental flux based on the chloride dosage at downstream or upstream of the electrodiffusion cell.

5. Conclusions

A new technique for exploitation of chloride electrodiffusion is proposed. It takes into account the electrocapillary phenomena that occur during the chloride transfer at the interface between wall pores and pores solution. Thus, the modelling had to be considered with electrical parameters like current densities, space charge densities and conductivities. Including the double layer effect on chloride transfer (expressed by the double layer capacity C_{SH} which can be found in the functions $f_1(\sigma,z)$ and $f_2(\sigma,z)$ through the parameter μ), the model allows calculating chloride flux from current densities obtained experimentally by chronoamperometry in the steady state.

An experimental validation was carried out by comparison between calculated values of flux and measured ones. A good correlation between the model results and the measurements was obtained. Calculating the flux in this way has the main advantage in avoiding inaccuracies of chloride dosage. Indeed, current measurements are more accurate and easier to obtain than measurements of chloride concentrations by dosage.

Thus, it is shown that this new method allows characterising more accurately and more easily the resistance of cement-based materials to the penetration of chloride ions.

However, these preliminary results have to be confirmed by other applications on different kinds of materials like mortars and concrete. Moreover, extending this model to non-steady state, i.e. when the current densities are decreasing (Fig. 4) seems to be desirable to understand the phenomena that could occur in this case.

Appendix A

Parameters in Eqs. (7) and (8):

$$\alpha_P = \frac{\sum_{k=1}^{s} Z_k^2 D_k C_k}{D_P C_P} \quad \alpha_N = \frac{\sum_{l=1}^{p} Z_l^2 D_l C_l}{D_N C_N}$$

Parameters in Eqs. (9) and (10):

$$D = \frac{(\alpha_P + \alpha_N) D_P D_N}{\alpha_P D_P + \alpha_N D_N} \quad D_S = \frac{2 D_{Na^+} D_{Cl^-}}{D_{Na^+} + D_{Cl^-}}$$

$$\lambda_S = \frac{D_S}{D} \quad \beta = \frac{\alpha_P D_P - \alpha_N D_N}{\alpha_P D_P + \alpha_N D_N}$$

$$\beta_S = \frac{D_{Na^+} - D_{Cl^-}}{D_{Na^+} + D_{Cl^-}} \quad \sigma_B^* = \frac{RT}{FD}\sigma_B \quad E^* = \frac{F}{RT}E$$

Parameters in Eqs. (11) and (12):

$$f_1(\sigma,z) = \frac{\sigma + \lambda_e\left[\sqrt{z^2 + 4\mu^2\sigma} - 2\mu\sigma^{1/2}\right]}{\left[\left\{\sigma + \lambda_e\left(\sqrt{z^2 + 4\mu^2\sigma} - 2\mu\sigma^{1/2}\right)\right\}^2 - \lambda_e^2 z^2\right]}$$

$$f_2(\sigma,z) = \frac{\lambda_e z}{\left[\left\{\sigma + \lambda_e\left(\sqrt{z^2 + 4\mu^2\sigma} - 2\mu\sigma^{1/2}\right)\right\}^2 - \lambda_e^2 z^2\right]}$$

where σ can take value of σ_B or that of σ_S,

$$\mu = \frac{(1-\beta^2)\sigma_B^*\delta_0}{C_{SH}EL} \quad \lambda_e = \frac{1}{\chi}\frac{\tau_C}{\tau_D} \quad \chi = \frac{RT}{FEL}$$

$$\beta_T = \frac{D_{PS} - D_{NS}}{D_{PS} + D_{NS}} \quad D_{PS} = \frac{D_P C_P + D_{Na^+} C_{Na^+}}{C_P + C_{Na^+}}$$

$$D_{NS} = \frac{D_N C_N + D_{Cl} C_{Cl^-}}{C_N + C_{Cl^-}}$$

C_P: concentration of anions (M), C_P: concentration of cations (M), C_{SH}: equivalent capacity of electrical double layer ($F\,m^{-2}$), D: global equivalent ionic diffusion coefficient before NaCl addition ($m^2\,s^{-1}$), D_s: equivalent ionic diffusion coefficient of sodium and chloride ($m^2\,s^{-1}$), E: applied electrical field ($V\,m^{-1}$), L: sample thickness (m), α_P, α_N: equivalent valence of ionic transfer for cations and anions, respectively, β: coefficient, which represents the gap between diffusion coefficients of ions, contained in the basic electrolyte, β_s: coefficient, which represents the gap between diffusion coefficients Na^+ and Cl^-, δ_0: thickness of electrical double layer (m), τ_C: time constant, which characterises the adsorption electrocapillary phenomena (s), τ_D: time constant, which characterises the diffusion process (s).

References

[1] El-Belbol SM. Acceleration of chloride ion diffusion in concrete. PhD Thesis, Imperial College, London, 1990.

[2] Tang L, Nilsson LO. Rapid determination of chloride diffusivity of concrete by applying an electrical field. ACI Mater J 1992; 89:49–53.

[3] Andrade C. Calculation of chloride diffusion in concrete from migration measurements. Cem Concr Res 1993;23:724–42.

[4] Zhang T, Gjørv OE. An electrochemical method for accelerated testing of chloride diffusivity in concrete. Cem Concr Res 1994; 24:1534–48.

[5] Streicher PE, Alexander MG. A chloride conduction test for concrete. Cem Concr Res 1995;25:1284–94.

[6] Onyejekwe OO, Reddy N. A numerical approach to the study of chloride ion penetration into concrete. Mag Concr Res 2000; 52:243–50.

[7] Truc O, Ollivier JP, Carcasses M. A new way for determining the chloride diffusion coefficient in concrete from steady state migration. Cem Concr Res 2000;30:217–26.

[8] Prince W, Ollivier JP, Truc O. Electrochemical aspects of the accelerated test of chloride ions permeability. Mater Struct 1999; 32:243–51.

[9] Chatterji S, Kawamura M. Electrical double layer, ion transport and reactions in hardened cement paste. Cem Concr Res 1992; 22:774–82.

[10] Marchand J, Gérard B, Delagrave A. Ions transport mechanisms in cement-based materials. Report GCS-95-07, University Laval, Canada, 1995.

[11] Amiri O. Modélisation de l'électrodiffusion des ions chlorures dans les mortiers de ciment—Intégration des phénomènes d'adsorption électrocapillaire. PhD Thesis, University of La Rochelle, 1998 (in French).

[12] Aït-Mokhtar A, Amiri O, Sammartino S. Analytic modelling and experimental study of the porosity and permeability of a porous medium—Application to cement mortars and granitic rock. Mag Concr Res 1999;51:391–6.

[13] Nilsson LO, Poulsen E, Sanberg P, Sorensen HE, Klinghffer O. Chloride penetration into concrete, state of the art, transport processes, corrosion initiation, tests methods and prediction models. Hetek report, 1996.

[14] Amiri O, Aït-Mokhtar A, Dumargue P. Optimisation de l'exploitation de l'essai d'électrodiffusion d'ions chlorures dans le béton. Revue Française de Génie Civil 2000;4:161–73.

[15] Bretton D, Ollivier JP, Ballivy G. Diffusivité des ions chlorures dans la zone de transition entre pâte de ciment et roche granitique. In: Proceedings of the RILEM International Conference. Toulouse: Chapman & Hall Editions; 1992. p. 269–278.